



*In the Name of Allah, The Most beneficiary,  
The Most Gracious, The Most Merciful*

*Theoretical Study of Steady Three  
Dimensional Stagnation Point Flow of  
Micropolar Nanofluid Past a Cylinder.*



By

*Nadeem Abbas.*

*Department of Mathematics  
Quaid-i-Azam University  
Islamabad, Pakistan  
2017*

*Theoretical Study of Steady Three  
Dimensional Stagnation Point Flow of  
Micropolar Nanofluid Past a Cylinder.*



By

*Nadeem Abbas*

Supervised By

*Dr. Sohail Nadeem.*

*Department of Mathematics  
Quaid-i-Azam University  
Islamabad, Pakistan  
2017*

*Theoretical Study of Steady Three  
Dimensional Stagnation Point Flow of  
Micropolar Nanofluid Past a Cylinder.*



By  
*Nadeem Abbas*

A DISSERTATION SUBMITTED IN THE PARTIAL FULFILLMENT OF THE REQUIREMENT

FOR THE DEGREE OF

MASTER OF PHILOSOPHY

IN

*MATHEMATICS*

*Supervised By*

*Dr. Sohail Nadeem.*

*Department of Mathematics*

*Quaid-i-Azam University*

*Islamabad, Pakistan*

*2017*

*This Thesis is dedicated to the Ideal personalities of my life,*

## *My Parents*

*Your memories will remain alive in our hearts forever.*

*The Thesis is also dedicated to the reason of my success,*

## *My Brother Ramzan*

*Thanks' for your love, encouragement and constant support while I was far away from home during my studies.*

# *Acknowledgement*

I start my acknowledgment to saying Thanks Almighty **Allah** for giving me strength, wisdom, confidence and perseverance to continue my studies, without His sufficient grace and mercy; I would not have been able to complete this work. After Almighty **Allah** I say thanks to the **Holly Prophet Hazrat Muhammad** (Peace be upon him) who emphasized the importance of knowledge by saying "Learn the knowledge from cradle to grave". After **Prophet (P.B.U.H)** I say thanks to **Holly Prophet family Imam Ali (a.s), Syeda Fatima (s.a), Imam Hassan (a.s), Imam Hussain (a.s)** and especially thanks to **Imam Zamana Hazrat Imam Mehdi (Alajl)** who's preaching's give encourage me to get the knowledge.

I Say thanks form the deepness of heart to my great teacher and kind supervisor, **Dr. Sohail Nadeem** for his expert guidance, constructive criticism, continuous encouragement and providing me with an excellent atmosphere for doing research. His guidance helped me in all the time of research and writing of this thesis. I could not have imagined having a better supervisor for my M.Phil. study. I would also like to thanks my all teachers who taught and bring me able to overcome all the challenges, Specially **Dr. Malik Muhammad Yousaf, Dr. Muhammad Afzal, Pro. M. Sirfaraz, Pro. M. Nawaz and Pro. Itrat Qurnain.**

I can't imagine completing my acknowledgment without considering my friends. Firstly, I am glad to acknowledge my senior lab fellow and my darling **Mr. Arif Ullah Khan, Mr. Noor Muhammad and Mr. Zahid Ahmad** whose kind suggestions are very helpful for me throughout my work. Then saying special thanks to my beloved friend and colleague I really enjoyed his company from beginning to end and tanks to other friends **Arsalan Hayyat, Noor ul Huda and M. Shafiq** and many more (it is not feasible to name all). Thanks for being around and sharing several good times together during my stay in the University.

Finally, I would like to thanks the personalities without them my life is incomplete and colorless, my **Parents, Brothers and Sisters.** I don't achieve any goal of my life without their everlasting love and blessings. Thank you **Abu G, Ami G and Bhai Jan** for endless supporting to achieve my desired goal. I consider myself the luckiest person in the world having such a supportive family, standing behind me with their love and affection.

*Nadeem Abbas*

# Theoretical Study of Steady Three Dimensional Stagnation Point Flow of Micropolar Nanofluid Past a Cylinder

By

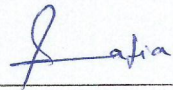
**Nadeem Abbas**

## CERTIFICATE

A THESIS SUBMITTED IN THE PARTIAL FULFILLMENT OF THE REQUIREMENTS FOR THE DEGREE OF THE MASTER OF PHILOSOPHY IN MATHEMATICS

We accept this thesis as conforming to the required standards

1. \_\_\_\_\_  
**Prof. Dr. Sohail Nadeem**  
(Supervisor)

2.  \_\_\_\_\_  
**Dr. Safia Akram**  
Associate Professor  
National University of Science  
and Technology, Rawalpindi.  
(External Examiner)

3. \_\_\_\_\_  
**Prof. Dr. Muhammad Yousaf Malik**  
(Chairman)

**Department of Mathematics**  
**Quaid-i-Azam University**  
**Islamabad, Pakistan**  
**2017**

# Preface

A fluid which consists of (1–100 nm) sized particles is called Nano-fluid. Nanofluids are engineered colloids made of a (1–100 nm) nanoparticles and base fluid (water). This is proved by the experiments which the thermal conductivity of nanofluids are greater as compare to the base fluids. Choi [1] was the first person who addressed about nanoparticle. Buongiorno [2] studied about the convective transport in nanofluids and gave a theoretical model. Main topic of studies which focus on the natural convection in inclusions having magnetic depicts have pondered an electrically conducting fluid with less thermal conductivity. Various interests of recent specialists are achieved by the nanofluids. In the real life, the common use of nanoparticles in nanofluids made of metals, carbon nanotubes oxides or carbides. Nanofluid is the combination of nanoparticles (including metals e.g. gold and copper, metal oxides e.g. alumina, zirconia, silica and titania, oxide ceramics e.g.  $Al_2O_3$  and  $CuO$ , metal carbides e.g.  $SiC$ , metal nitrides e.g.  $SiN$ ,  $AlN$ , carbon e.g. graphite) and base fluids (including water, oils, biofluids, polymeric solutions, organic liquids e.g. ethylene, triethylene-glycols, refrigerants etc.). Actually, fluid is used in various engineering and industrial processes. The several applications of the nanofluids are used very common in the fields of communication, electronics, high-power x-rays, optical devices, material processing, laser etc. Some recent researches on the flow of nanofluids are experimented [3 – 4]. Nadeem and Lee [5] have been enlarged the idea of nanofluid over an exponentially stretching sheet.

A subclass of microfluidic is called micropolar fluid, the idea was addressed by Eringen [6, 7]. The natural convective flow model of micropolar nanofluid was presented by Bourantas et al. [8]. Buongiorno [9] was worked on convective transport in nanofluids. Most of the researchers



interested to study the theory of micropolar fluids. The theory mentioned non-Newtonian fluid model is important to discuss fluid behavior of lubricants, colloidal fluids, liquid crystals and suspension fluids which cannot be determined by the classical Newtonian fluid. In the absence of smoke or dust, exclusively in a gas might likewise be revealed utilizing micropolar liquid model. MHD micropolar stagnation point flow fluid towards heat surface and stretching sheet have been addressed by Ashraf and Ashraf [10]. Many actions in engineering fields appear at large temperature. The awareness of radiation heat transfer becomes very important for the pattern of pertinent material. Many researchers like Nazar et al. [11], Yücel [12], Lok et al. [13], Alomari et al. [14], Ishak et al. [15] and Yacob et al. [16] and Takhar et al. [17] have been worked on micropolar fluid by considering some different physical aspects. Rauf et al. [18] was also worked on the effect of hydromagnetic micropolar fluid restricted to stretchable disk. Siddiq et al. [19] was worked on the impact of convective radiation in magnetic hydrodynamics micropolar stagnation point flow fluid towards a shrinking sheet. In a permeable channel, the impact of heat transfer and micropolar fluid flow was presented by Sheikholeslami et al. [20]. In three dimensional numeric results of magnetic hydrodynamics micropolar stagnation point flow fluid was coined by Borrelli et al. [21].

The basic fluids flow which impinge on a solid surface, called stagnation point flow. Wang [22] was addressed the exact similarity solution of Navier Stokes equations in the stagnation point region. The classical study include the two dimensional stagnation point flow was coined by Hiemenz [23]. Homann [24] was addressed the axisymmetric stagnation point flow. Nazar et al. [25] was addressed the unsteady boundary layer flow in a stagnation point over stretching sheet. The impact of slip and thermal radiation at the stagnation point flow over stretching sheet is coined by Nadeem et al. [26]. In the convective boundary condition, the impact of radiation on

MHD stagnation point flow of nanofluid over stretching surface is studied by Nadeem et al. [27]. In the area of stagnation point over stretching sheet, unsteady boundary layer flow was addressed by Pop et al. [28].

The main theme of present work is to discuss the effect of magnetic hydrodynamics micropolar fluid in the absence of stagnation point flow at a circular cylinder having sinusoidal radius variation. Impacts of micropolar, nanoparticle and MHD also take into account. Using the transformation equations, the system of governing partial differential equations are reduced to the system of nonlinear ordinary differential equations. The system of ordinary differential equations are solved numerically by fifth order Runge-Kutta-Fehlberg method. The impact of physical parameters on velocities, angular velocities and temperature profiles are shown in graphical and tabular form.

# Contents

<b>Chapter 1</b> .....	7
<b>1 Basic definitions</b> .....	7
1.1 Fluid .....	7
1.1.1 Fluid mechanics .....	7
1.1.2 Fluid dynamics .....	7
1.1.3 Fluid statics .....	8
1.2 Classification of fluids .....	8
1.2.1 Inviscid fluid .....	8
1.2.2 Viscous fluid .....	8
1.2.3 Newtonian Fluids .....	8
1.2.4 Non Newtonian fluids .....	9
1.3 Stress .....	10
1.3.1 Shear Stress .....	10
1.3.2 Normal Stress .....	10
1.4 Density .....	10
1.5 Dimensionless numbers .....	11
1.5.1 Skin friction .....	11
1.5.2 Reynolds number .....	11
1.5.3 Nusselt Number .....	12
1.5.4 Prandtl Number .....	12
1.6 Nanofluids .....	13
1.7 Micropolar Fluids .....	13
1.8 Magneto-Hydrodynamics .....	13
1.9 Basic equations .....	14
1.9.1 Continuity equation .....	14
1.9.2 Energy equation .....	14
1.9.3 Momentum equation .....	15
1.9.4 Micropolar equation .....	16
1.10 Heat transfer .....	16

1.11	Boundary layer .....	17
<b>Chapter 2</b>	.....	18
2.1	Introduction .....	18
2.2	Flow structure.....	18
2.3	Results and discussions .....	22
2.4	Closing Remarks.....	28
<b>Chapter 3</b>	.....	29
3.1	Introduction .....	29
3.2	Flow Structure .....	29
3.3	Nusselt number and Skin friction coefficient .....	33
3.4	Results and discussion .....	34
3.5	Final remarks .....	45
3.6	References .....	46

# Chapter 1

## 1 Basic definitions

This chapter contains some essential definitions, concepts and laws which are beneficial for the thoughtful of analysis accessible in the resultant chapters.

### 1.1 Fluid

Material that flows permanently and continuously in direction of shear stress (the ratio of stress force and area under the action) regardless how it is small, called fluids. It is also referred to be a fluid which defines as a word substance in liquid and gas phase.

#### 1.1.1 Fluid mechanics

Mechanics is a science, deals the study of the nature and properties of fluids at stationary position or in moving state. There are two main subclasses of fluid mechanics.

(1) Fluid dynamics

(2) Fluid statics

#### 1.1.2 Fluid dynamics

The study about the flow of fluid in liquids and gases is called fluid dynamics (is a sub branch of fluid mechanics).

### 1.1.3 Fluid statics

A branch of fluid mechanics that deal with the study about the flow of fluid at rest is called fluid statics.

## 1.2 Classification of fluids

### 1.2.1 Inviscid fluid

Inviscid fluid is a fluid which has negligible (zero viscosity) viscosity or  $\mu = 0$  due to constant density and vanished in nature. It suggests negligible viscosity ( $\mu = 0$ ) with no internal resistance. Such types of the fluids are called inviscid fluids. While gases are considered as ideal fluids.

### 1.2.2 Viscous fluid

A viscous fluid is a fluid that has finite or non-zero viscosity ( $\mu \neq 0$ ), are also called real fluid. When fluid can expend a tangential stress on the surface, is in contact with the surface. Such fluids can be divided into two types such as compressible and incompressible.

### 1.2.3 Newtonian Fluids

A real or non-viscous fluid in such a way that the rate of shear stress is directly proportional to its deformation rate at every point which satisfy the Newton's law of viscosity. These fluids resist against deformation and flow freely. Mathematically, defined as

$$\tau^* = \mu^* \frac{du}{dy}$$

Here,  $\mu^*$  is shear viscosity of fluid (Proportionality constant),  $\tau^*$  is shear stress acting on a plane normal to  $y$  –direction and  $u$  is the velocity of fluid in  $x$  –direction. Common examples of Newton’s fluids are water, gases like air, light hydrocarbon oils, gasoline, sugar solutions and mineral spirit etc.

#### 1.2.4 Non Newtonian fluids

A fluid is called non-Newtonian fluid that does not fulfil the Newton’s law of viscosity and shear stress is directly and non-linearly proportional to the strain rate (the derivative of its deformation over time).

$$\tau^* = \varepsilon^* \frac{du}{dy},$$

$$\varepsilon^* = k \left( \frac{du}{dy} \right)^{n-1},$$

$$\tau^* = k \left( \frac{du}{dy} \right)^n, n \neq 1,$$

Here,  $k$  is the flow behavior index,  $\varepsilon^* = k \left( \frac{du}{dy} \right)^{n-1}$  is apparent viscosity and  $n$  is consistency index. The above equation will be reduced (by using  $k = \mu^*$  and  $n = 1$ ) into Newtonian’s law of viscosity. Blood, grease, paints, toothpaste, ketchup and gels, etc. are the examples of non-Newtonian fluids.

## 1.3 Stress

In continuum mechanics, stress is interpreted as a physical quantity which demonstrated the internal forces between the neighboring particles of a continuous substance. In SI system, the unit of stress is ( $\text{kg}/\text{m}\cdot\text{s}^2$ ) and its dimension is ( $\frac{\text{M}}{\text{LT}^2}$ ). Stress has further two branches such as the shear stress and normal stress.

### 1.3.1 Shear Stress

Shear stress is the component of stress acting parallel to the unit surface area of the continuous substance (resisting force per unit area). The mathematical forms of shear stress is

$$\tau = \frac{\text{Force (resisting)}}{\text{Area}}$$

### 1.3.2 Normal Stress

Normal stress is the component of stress acting perpendicular to the unit surface area of the continuous substance.

## 1.4 Density

The volumetric density or simply the density of a fluid is defined as mass contain unit per volume. It is represented by a Greek letter rho ( $\rho$ ) and can be defined mathematically as

$$\text{Density} = \rho = M/V$$



## 1.5 Dimensionless numbers

### 1.5.1 Skin friction

Friction produces between moving fluid and solid surface, called skin friction. It can also define as the friction due to the viscous resistance at the boundary in the flow. In mathematically

$$C_f = \frac{\tau_w}{\rho_f U_w^2},$$

Where the surface shear stress, density of fluid and velocity at wall are defined as respectively  $\tau_w$ ,  $\rho_f$  and  $U_w$ . It effects on flow characteristics which reduce skin friction in laminar flow and increase skin friction in turbulent flow.

### 1.5.2 Reynolds number

In the beginning, Stokes was the first person who introduced the Reynolds number. Reynolds number ( $Re$ ) is a quantity (dimensionless number) that describes the behavior of flow (turbulent or laminar) which defined as the ratio of inertial force ( $V \cdot \rho$ ) to viscous forces ( $\mu/L$ ). The flow can be easily determined (flow is turbulent or laminar) with the help of Reynolds number. If the flow is laminar when the viscous forces are dominant for low Reynolds number ( $Re < 2300$ ). The flow is turbulent when the viscous forces are dominant for high Reynolds number ( $Re > 4000$ ). Mathematically

$$Re = \frac{\text{Inertial force}}{\text{Viscous force}} = \frac{L}{v}$$

Where the kinematic viscosity is  $\nu$ , the characteristics of flow range is  $L$ .

### 1.5.3 Nusselt Number

Nusselt number (Nu) is dimensionless quantity, used in heat transfer and defines as ratio of the heat convection to heat conduction transfer across (normal) to the boundary. It was introduced, German mathematician Nusselt. Mathematically, it is defined as

$$\text{Nu} = \frac{\text{Total heat transfer}}{\text{Conductive heat transfer}},$$

$$\text{Nu}_x = \frac{h_x x}{k},$$

Where  $k$  represents the thermal conductivity of fluid,  $h_x$  represents conductive heat transfer coefficient and  $x$  represents the characteristics of flow range.

### 1.5.4 Prandtl Number

A dimensionless number which describes the ratio of momentum diffusivity to thermal diffusivity. Physically, it gives the relation between momentum boundary layer thickness and thermal boundary layer thickness. For small Pr., the heat diffuses rapidly as compare to momentum. It can be defined mathematically, as fellow

$$\text{Pr} = \frac{\text{viscous diffusion rate}}{\text{thermal diffusion rate}},$$

$$\text{Pr} = \frac{\nu}{\alpha} = \frac{\mu/\rho}{k/\rho c_p} = \frac{\mu c_p}{k},$$

Where,  $\alpha$  represents the thermal diffusivity,  $\nu$  represents the momentum diffusivity or kinematic viscosity,  $c_p$  represents the specific heat capacity and  $k$  represents the thermal conductivity.

## 1.6 Nanofluids

A fluid which restricted in a nanoscale structure, is called nanofluids. The nanoparticles are used in nanofluids, are mostly made of metals, oxides, carbon nanotubes or carbides and ethylene glycol, water, oil, etc. are mostly used as a base fluid. Effective density, effective dynamic viscosity and thermal conductivity, is involved in the fluid flow and heat transfer phenomena of nanofluid transform properties.

## 1.7 Micropolar Fluids

A fluid which contains of rigidly and randomly oriented particles suspended in viscous region is called micropolar fluids, where the deformation of fluid particles is disregarded. The characteristic of micropolar fluid particles having spin inertia as well as rotational the element of a micropolar fluid can shrink or expand independently and undergoes into the rotation. There are good examples of micropolar fluids namely liquid crystals and animal blood. Eringen [6] was the first person who proposed the model of micropolar fluid, is a principal of classical Navier Stokes fluid model. The stress tensor is not symmetric in micropolar fluid model and unlike the Navier Stokes model but it can support body torque and couple stress.

## 1.8 Magneto-Hydrodynamics

The properties of electrically conducting fluids study of magnet is called magneto-hydrodynamics. Usually example of MHD are plasmas, liquid metals, salt water and

electrolytes. The general concept of MHD, magnetic fields can induce currents in a moving conductive fluid whatever in turn polarizes the fluid and reciprocally changes the magnetic field by itself.

## 1.9 Basic equations

### 1.9.1 Continuity equation

An equation which represents the law of mass conservation. The law of mass conservation means the rate of mass enter into the system is equal to rate of mass leave the system. The continuity equation can be written in the “differential form”

$$\frac{\partial \rho}{\partial t} + \vec{\nabla} \cdot (\rho \vec{V}) = 0,$$

Where,  $\vec{V} = \vec{V}(u, v, w)$  is velocity flow of the fluid and  $\rho$  is the fluid density.

$\vec{\nabla}$  is an operator defined as

$$\vec{\nabla} = \frac{\partial}{\partial x} \underline{i} + \frac{\partial}{\partial y} \underline{j} + \frac{\partial}{\partial z} \underline{k},$$

Here  $\underline{i}$ ,  $\underline{j}$  and  $\underline{k}$  are unit vectors. In case of an incompressible fluid, the continuity equation reduces into the following form

$$\vec{\nabla} \cdot \vec{V} = 0.$$

### 1.9.2 Energy equation

The energy equation is

$$(\rho C_p)_{nf} \frac{d\vec{T}}{dt} = \tau \cdot \vec{L} + k_{nf} \vec{\nabla}^2 \vec{T} - \text{div} q_r$$

Where,

$\rho$  = Density of fluid

$\vec{L}$  = Gradient of velocity

$q_r$  = Radiative heat transfer

$t$  = Time &  $\vec{T}$  = Temperature

$k_{nf}$  = Thermal conductivity of nanofluids

$(\rho C_p)_{nf}$  = Heat capacity of nanofluids

### 1.9.3 Momentum equation

The equation of motion for nanofluid is

$$\rho \frac{d\vec{V}}{dt} = \vec{\nabla} \cdot \vec{S} + \rho \vec{B},$$

Where, the velocity vector in three dimensional space is  $\vec{V} = \vec{V}(u, v, w)$ , the body force is represented as “ $\vec{B}$ ”, the identity tensor is represented as “ $\vec{I}$ ”, the dynamic viscosity “ $\mu$ ” and “ $\vec{S}$ ” is the Cauchy stress tensor which is defined as

$$\vec{S} = -p\vec{I} + \mu \vec{A}_1$$

In which

$$\vec{A}_1 = \text{grad}\vec{V} + (\text{grad}\vec{V})^T,$$

Here  $\vec{A}_1$  represents the first Rivlin Ericksen tensor which the grad of the velocities field is computed as

$$\text{grad}\vec{V} = \begin{pmatrix} \frac{\partial u}{\partial x} & \frac{\partial u}{\partial y} & \frac{\partial u}{\partial z} \\ \frac{\partial v}{\partial x} & \frac{\partial v}{\partial y} & \frac{\partial v}{\partial z} \\ \frac{\partial w}{\partial x} & \frac{\partial w}{\partial y} & \frac{\partial w}{\partial z} \end{pmatrix}$$

#### 1.9.4 Micropolar equation

Generalization of momentum equations for micropolar fluid is given as

$$\rho \frac{D\vec{V}}{Dt} = -\vec{\nabla}p + (\mu + k_1)\vec{\nabla}^2\vec{V} + k_1 * (\vec{\nabla} \times \vec{N}) + \vec{J} \times \vec{B},$$

$$\rho J * \frac{D\vec{N}}{Dt} = \gamma * \vec{\nabla}^2\vec{N} + k_1(-2\vec{N} + \vec{\nabla} \times \vec{V}),$$

#### 1.10 Heat transfer

It is the exchange of thermal energy from one system to another is called heat transfer.

Three ways that heat can be transfer, namely convection (by fluid movement), conduction (by direct contact) and radiation (by electromagnetic waves).

## 1.11 Boundary layer

German astronomer “Ludwig Prandtl” gave the concept of boundary layer in 1904, in his article which he presented in mathematical congress. The thickness of the boundary layer is taken from surface to point at which velocity is 99% of the free stream velocity. This approach helps us to reduce equations because the solution of the Navier-Stokes equation is exclusive. So these equations do not subscribe in the field of aerodynamics, viscous fluid dynamics and ship-hulls for different decades until the concept of boundary layer approximation were described. In the boundary layer approximations, the Navier-Stokes equations are examined and terms which do not subscribe significantly are dropped. This process evolves the model equations to rather reasonable and simple shape.

## Chapter 2

# Steady three dimensional stagnation point flow of nanofluid towards a circular cylinder having sinusoidal radius variation

### 2.1 Introduction

The theme of present chapter is to examine the impact of stagnation point flow of nanofluid passing through a circular cylinder having sinusoidal radius variation. In the present discussion, three varieties of nanoparticles are taken into account namely, Titania, Copper and Alumina having base fluid water. Reducing the system of partial differential equation into ordinary differential equation by applying similarity transformation. These ordinary differential equations are solved by fifth order Runge-Kutta-Fehlberg method. Effect of various parameters are addressed in the tabular and graphically forms.

### 2.2 Flow structure

Consider the three-dimensional stagnation point flow of nanofluid towards a circular cylinder having sinusoidal radius variation as revealed in **Fig. 2.1**. There is a stagnation point on the cylinder at each minimum and maximum of the radii (points M, N and O). From M to N and O to N there is a connection line separating the flow that goes on the side of the cylinder. The



equation of streamline can formulate like  $x = \beta y^{1/c}$ , where the fraction of the gradient of stream velocities is  $c$  and defined as  $c = \frac{b^*}{a^*}$  and  $\beta$  is constant, which gives a particular streamline.

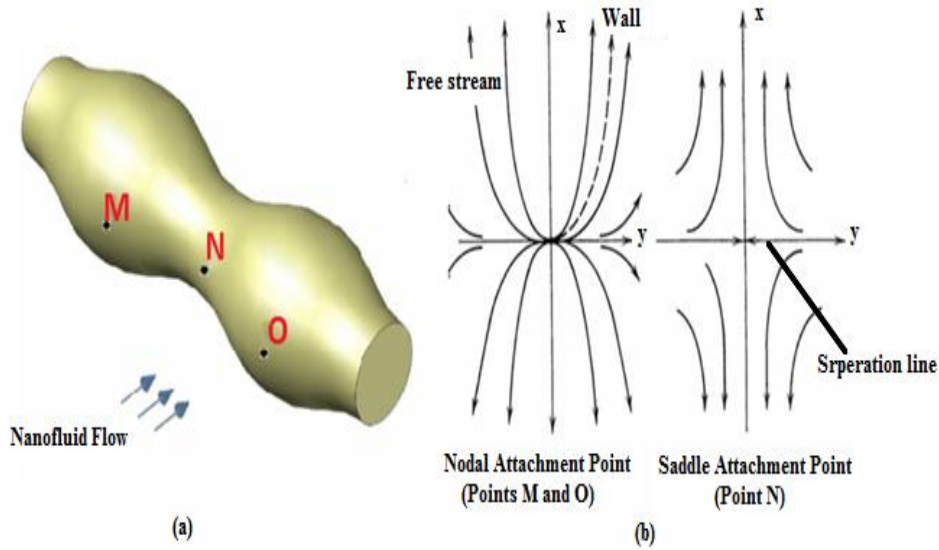


**Fig 2.1. (a):** The diagram of circular cylinder having sinusoidal radius variation.

**Fig 2.1. (b):** Streamlines pattern on the surface.

The range of saddle and nodal stagnation points respectively are  $-1 \geq c \geq 0$  and  $0 \geq c \geq 1$ . In the absence of external mechanical body force, the flow equations are

$$\frac{\partial u^*}{\partial x} + \frac{\partial v^*}{\partial y} + \frac{\partial w^*}{\partial z} = 0 \quad 2.2.1$$

In component form the equations are defined as

$$u^* \frac{\partial u^*}{\partial x} + v^* \frac{\partial u^*}{\partial y} + w^* \frac{\partial u^*}{\partial z} = a^{*2} x + v_{nf} \frac{\partial^2 u^*}{\partial z^2} \quad 2.2.2$$

$$u^* \frac{\partial v^*}{\partial x} + v^* \frac{\partial v^*}{\partial y} + w^* \frac{\partial v^*}{\partial z} = b^{*2} y + \nu_{nf} \frac{\partial^2 v^*}{\partial z^2} \quad 2.2.3$$

The energy equation can be written as

$$u^* \frac{\partial T^*}{\partial x} + v^* \frac{\partial T^*}{\partial y} + w^* \frac{\partial T^*}{\partial z} = \alpha_{nf} \frac{\partial^2 T^*}{\partial z^2} \quad 2.2.4$$

Boundary condition are given as

$$\begin{aligned} u^* = 0, \quad v^* = 0, \quad w^* = 0, \quad T^* = T_s^* \quad \text{at } z \rightarrow 0, \\ u^* \rightarrow ax, \quad v^* \rightarrow by, \quad T^* \rightarrow T_\infty^*, \quad \text{at } z \rightarrow \infty, \end{aligned} \quad 2.2.5$$

where ‘ $u^*$ ,  $v^*$  and  $w^*$  are the velocity components along  $x$  – ,  $y$  – and  $z$  – direction respectively,  $T^*$  is the temperature distribution,  $\rho_{nf}$  is the density of nanofluid, nanofluids dynamic viscosity is  $\mu_{nf}$ ,  $k$  is the vortex viscosity,  $T_s^*$  is the constant wall temperature,  $T_\infty^*$  is the ambient temperature,  $a^*$  and  $b^*$  are constant ( $> 0$ ).

$$\mu_{nf} = \frac{\mu_f}{(1 - \phi)^{2.5}}, \quad Pr = \frac{\nu}{\alpha}, \quad \rho_{nf} = (1 - \phi)\rho_f + \phi\rho_s,$$

$$\alpha_{nf} = \frac{\kappa_{nf}}{(\rho C_p)_{nf}}, \quad (\rho C_p)_{nf} = (1 - \phi)(\rho C_p)_f + \phi(\rho C_p)_s,$$

$$\frac{\kappa_{nf}}{\kappa_f} = \frac{(\kappa_s + 2\kappa_f) - 2\phi((\kappa_s - \kappa_f))}{(\kappa_s + 2\kappa_f) + \phi((\kappa_s - \kappa_f))}.$$

Introducing the following transformable variables

$$\left\{ \begin{array}{l} \eta = z \sqrt{\frac{v_f}{a^*}}, u^* = a^* x f'(\eta), \\ v^* = b^* y g'(\eta), \\ w^* = -\sqrt{a^* v_f} (f + c g), \\ T^* = T_\infty^* + (T_s^* - T_\infty^*) \theta(\eta). \end{array} \right. \quad 2.2.6$$

The governing equations and related boundary conditions are transformed into following system of ordinary differential equations

$$\left( \frac{1}{(1-\phi)^{2.5} \left( 1 - \phi + \phi \frac{\rho_s}{\rho_f} \right)} \right) f''' + (c g + f) f'' - f'^2 + 1 = 0, \quad 2.2.7$$

$$\left( \frac{1}{(1-\phi)^{2.5} \left( 1 - \phi + \phi \frac{\rho_s}{\rho_f} \right)} \right) g''' + (c g + f) g'' - c g'^2 + c = 0, \quad 2.2.8$$

$$\frac{\frac{K_{nf}}{K_f}}{\text{Pr} \left( 1 - \phi + \phi \frac{(\rho C_p)_s}{(\rho C_p)_f} \right)} \theta'' + (c g + f) \theta' = 0, \quad 2.2.9$$

$$\left\{ \begin{array}{l} f(0) = 0, \quad f'(0) = 0, \quad f'(\infty) = 1, \\ g(0) = 0, \quad g'(0) = 0, \quad g'(\infty) = 1, \\ \theta(0) = 1, \quad \theta(\infty) = 0. \end{array} \right. \quad 2.2.10$$

Here  $f$  and  $g$  represents the modified velocity parameters,  $\theta$  represents the temperature prime denotes derivative with respect to  $\eta$ .

Two main essential physical quantities of present research are skin friction coefficient  $C_{fx}$  and  $C_{fy}$  along the  $x$ - and  $y$ - direction respectively and the local Nusselt number, which are characterize as below

$$C_{fx} = \frac{\tau_{wx}}{\rho_f u_w^2}, \quad C_{fy} = \frac{\tau_{wy}}{\rho_f u_w^2}, \quad Nu_x = \frac{xq_w}{k_f(T_w - T_\infty)}, \quad 2.2.11$$

These equations  $\tau_{wx}$  and  $\tau_{wy}$  are the shear stress surface in the  $x$  – and  $y$  – directions respectively. The  $q_w$  represents as the surface heat flux, the quantities are listed as follow

$$\begin{aligned} \tau_{wx} &= [(\mu_{nf}/\mu_f) \partial u^* / \partial z]_{z=0} & \tau_{wy} &= [(\mu_{nf}/\mu_f) \partial v^* / \partial z]_{z=0}, \\ q_w &= -k_{nf} (\partial T^* / \partial z)_{z=0}. \end{aligned} \quad 2.2.12$$

From equation (2.2.11) and (2.2.12), we get

$$\begin{aligned} Re_x^{1/2} C_{fx} &= \frac{1}{(1 - \phi)^{2.5}} f''(0), \\ (x/y) Re_x^{-1/2} C_{fy} &= \left( \frac{c}{(1 - \phi)^{2.5}} \right) g''(0), \\ Re_x^{-1/2} Nu_x &= -\frac{k_{nf}}{k_f} \theta'(0). \end{aligned}$$

where  $Re = \frac{ax}{v_{nf}}$  is the local Reynolds number.

## 2.3 Results and discussions

The system of nonlinear coupled differential equations (2.2.7 – 2.2.9) subject to the boundary conditions (2.2.10) have been solved numerically by using fifth order Runge-Kutta-Fehlberg method. In this present study, three kinds of nanoparticles have been discussed, namely alumina ( $Al_2O_3$ ), titanium dioxide ( $TiO_2$ ) and copper (Cu) with water as base fluids. Value of nanoparticle volume fractions are taken into account as  $0 \leq \phi \leq 0.2$ . According to the Yazdi [31] which shown in **Table 2.1**, it can also observed that  $TiO_2$  nanoparticle has the least value of thermal conductivity as to  $Al_2O_3$  and Cu because lesser heat transfer rate can be revealed by  $TiO_2$ . From the **Table 2.2**, the distinction in the local Nusselt number and the coefficient of skin-friction for several

nanoparticles due to conversion in solid particle  $\phi$  at the saddle point ( $c = 0.5$ ) is revealed. We have enumerated numerical results using numerical technique fifth order Runge-Kutta-Fehlberg method. In our study, three distinct nanoparticles namely, titania, copper and alumina are discussed. It is seen that the skin fraction coefficient in the direction of x- and y- axis improves with increase in nanoparticles volume fraction. While the heat transfer rate and solid nanoparticles have the same behavior of increasing. The improvement in Nusselt number is greater for copper and lesser for titania nanoparticle, it is observed. As the comparison of copper to conduct heat is higher than alumina but copper does not have the capacity to exchange heat greater than alumina. Thus, for increment of nanoparticle volume fraction transfer rate thermal energy large for the case of copper nanoparticle. **Figs.** [(2.2) – (2.3)] describe the distribution of the nanofluids velocity profiles respectively  $f'(\eta)$  and  $g'(\eta)$  for solid particles (nanoparticles volume fraction)  $\phi$ . **Fig.** 2.2 depicts the effect of solid particles  $\phi$  on the nanofluids velocity profile  $f'(\eta)$ , while  $\phi$  (solid nanoparticles) augment with slow down nanofluid velocity profile  $f'(\eta)$  at the critical points such that  $c = 0.5$  and  $c = -0.5$ .

**Fig.** 2.3 reveals the variation of nanofluids velocity profile  $g'(\eta)$  for several values of  $\phi$  (solid particles). The nanofluid velocity distribution  $g'(\eta)$  slow down with augment of  $\phi$  (solid nanoparticles) at the critical points such that  $c = 0.5$  and  $c = -0.5$ . In **Fig.** 2.4, an exposition of temperature profile  $\theta(\eta)$  with  $\eta$  for different values of nanoparticles volume fraction ( $\phi$ ) is clarified. It can be seen that nanoparticle volume fraction declined with improvement in temperature profile at nodal and saddle point near surface. **Figs.** 2.5, 2.6 and 2.7 reveal the effect of various nanoparticle densities (namely,  $\text{TiO}_2$ , Cu and  $\text{Al}_2\text{O}_3$ ) on temperature and velocities distributions at nodal and saddle points. While the behavior of velocity distributions offers large values of copper-water and lesser values for alumina-water which are shown in **Figs.** 2.5 and 2.6

at each critical points  $c = 0.5$  and  $c = -0.5$ . It is also seen in **Fig. 2.7**, the behavior of temperature profile is lesser for  $\text{Al}_2\text{O}_3$  – water and higher for Cu – water at the surface for both saddle and nodal points.

**Table 2.1:** Thermophysical characteristics of nanoparticles and fluid [29].

Thermophysical properties	Fluid phase (water)	$\text{Al}_2\text{O}_3$	$\text{TiO}_2$	Cu
$C_p$ (j/kg)K	4179	765	686.2	385
$\rho$ (kg/m <sup>3</sup> )	997.1	3970	4250	8933
k(W/mK)	0.613	40	8.9538	400
$\alpha \times 10^7$ (m <sup>2</sup> /s)	1.47	131.7	30.7	1163.1

**Table 2.2:** Skin friction and Nusselt number.

Nanoparticles		$\text{Re}_x^{-1/2} \text{Nu}_x$	$\text{Re}_x^{1/2} C_{fx}$	$\text{Re}_x^{1/2} C_{fy}$
	$\phi$	Numerical	Numerical	Numerical
$\text{TiO}_2$	0.0	1.4348	1.5254	0.6357
	0.1	1.5953	1.6642	0.6556
	0.2	1.6906	2.1524	0.8480
	0.3	1.8820	2.7832	1.0964
	0.4	2.0713	3.6424	1.4350
Cu	0.0	1.4348	1.5254	0.6357
	0.1	1.6179	1.9367	0.7630
	0.2	1.9290	2.6985	1.0619
	0.3	2.2474	3.6417	1.4346
	0.4	2.5876	4.9072	1.9331
$\text{Al}_2\text{O}_3$	0.0	1.4348	1.5254	0.6357
	0.1	1.5292	1.6466	0.6487
	0.2	1.7670	2.1155	0.8334
	0.3	2.0125	2.7234	1.0728
	0.4	2.2719	3.5525	1.3996

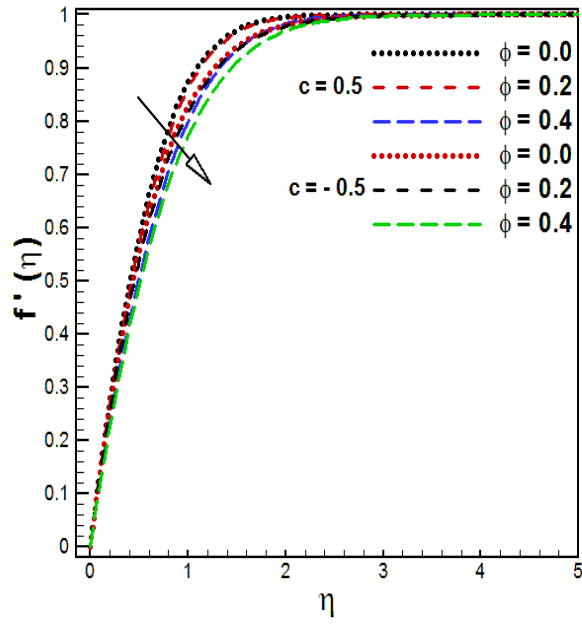


**Fig. 2.2:** Effect of  $\phi$  on velocity distribution

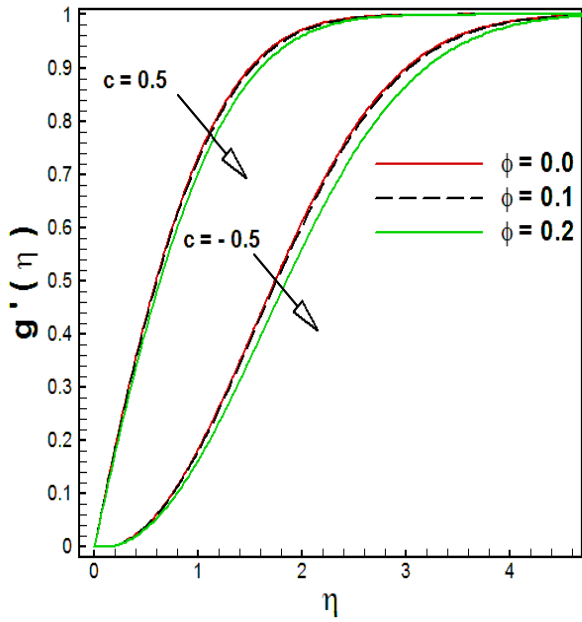


**Fig. 2.3:** Effect of  $\phi$  on velocity distribution.

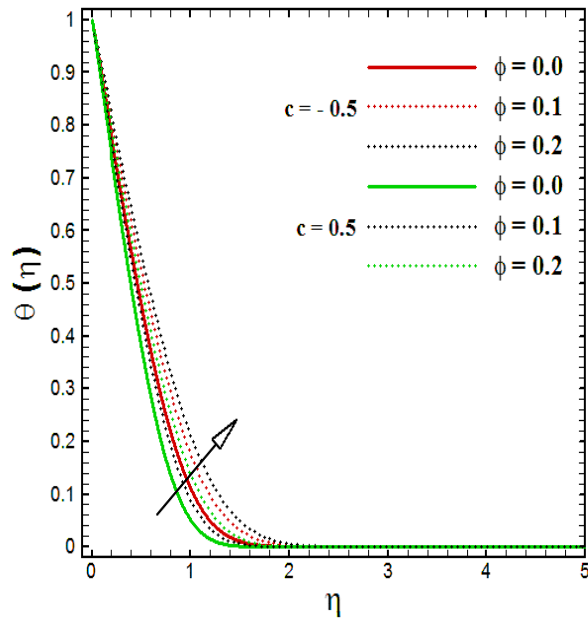


**Fig. 2.4:** Effect of  $\phi$  on temperature distribution.

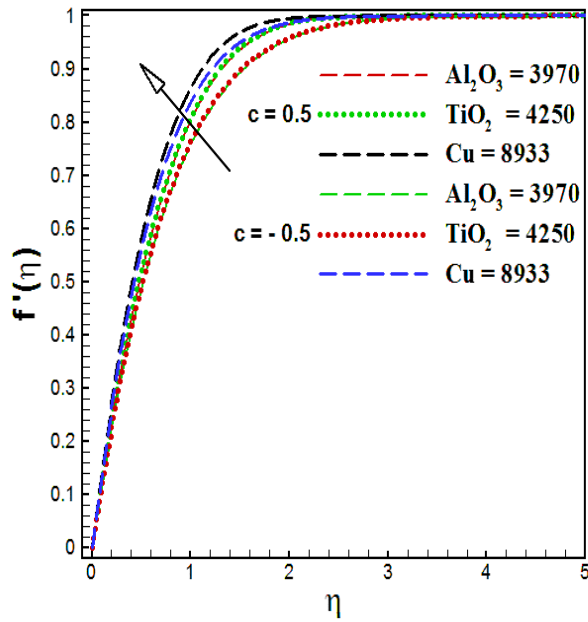


**Fig. 2.5:** Effect of densities on velocity distribution.



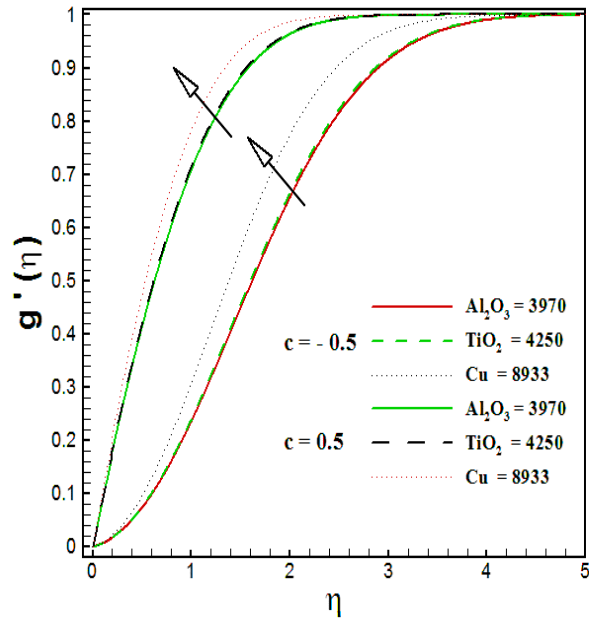


**Fig. 2.6:** Effect of densities on velocity distribution.

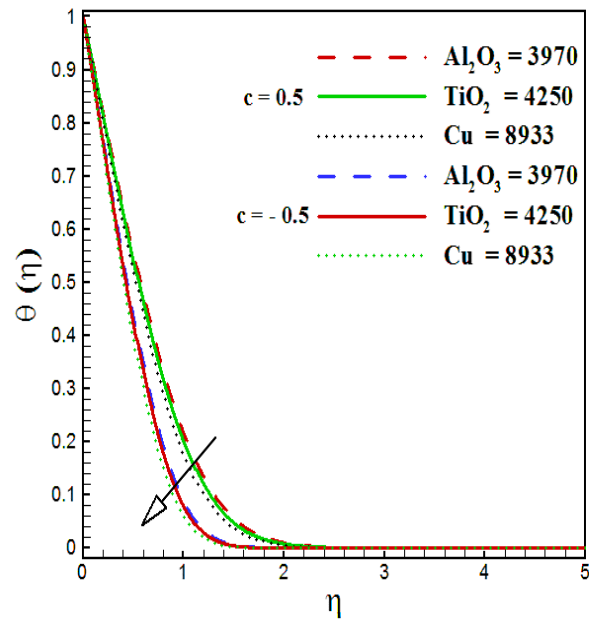


**Fig. 2.7:** Effect of densities on temperature distribution.

## 2.4 Closing Remarks

In our review study, the flow of nanofluid toward stagnation point over a circular cylinder having wavy radius. This problem has been solved by the numerical technique. Three categories of nanoparticle are investigated with water. From our investigation, we obtained the following remarks.

- I. It is seen that the temperature field and nanoparticle volume fraction have same behavior of increasing at nodal and saddle stagnation point.
- II. In our review, the velocity components in the direction of x- and y-axis reduce due to improvement in nanoparticle volume fraction at both critical points  $c = 0.5$  and  $c = -0.5$ .
- III. It is also seen that the behavior of nanoparticle volume fraction, the skin friction and rate of heat transfer have same increasing all through at nodal stagnation point.
- IV. Nusselt number and skin friction impediment reveals largest values for Cu-water as compare to Alumina- and Titania-water at the surface.
- V. The behavior of nanoparticle densities ( $\text{TiO}_2$ ,  $\text{Al}_2\text{O}_3$  and Cu) reveal the effect on velocity along x- and y-directions have larger for copper-water and lesser for alumina-water at nodal and saddle stagnation point.
- VI. The fact that Cu-nanoparticles possibly useful in the increment of heat transfer as compared to other nanoparticles in the study.

## Chapter 3

# Numerical study of MHD three-dimensional stagnation point flow of a micropolar nanofluid past a circular cylinder with sinusoidal radius variations

### 3.1 Introduction

In this chapter, the MHD effects are analyzed on the three-dimensional stagnation point flow of micropolar nanofluid. Three different nanoparticle namely Copper ( $Cu$ ), Titania ( $TiO_2$ ) and Alumina ( $Al_2O_3$ ) are compared considering water as a base fluid. The physical parameters are discussed near the saddle and nodal point on the circular cylinder having sinusoidal radius variation. Reducing the system of partial differential equation into ordinary differential equation by applying similarity transformations. These ordinary differential equations are solved by fifth order Runge-Kutta-Fehlberg method. Numerical data have been composed and deliberated for nusselt's number and skin friction coefficient. It is seen that the coefficient of skin friction and the heat transfer on the surface of cylinder are greater for copper–water nanofluid as compare to titania–water and alumina–water nanofluids.

### 3.2 Flow Structure

Consider the three-dimensional stagnation point flow of an electrically conducting incompressible micropolar nanofluid towards a circular cylinder having sinusoidal radius variation as shown in *Fig. 2.1*. The flow parameters are discussed near the saddle and nodal points. The saddle and

nodal points are simply correlated with the free stream parameter  $c$  that is  $c = 0$  which represents the flow over a plane,  $-1 < c \leq 0$  represents the nodal points and  $0 < c \leq 1$  represents the saddle point. There is a stagnation point on the cylinder at each maximum and minimum of the radius (points M, N and O). From M to N and O to N there is a connection line separating the flow that goes on either side of the cylinder. The equation of streamline can formulate like  $x = \beta y^{1/c}$ , where the fraction of the gradient of stream velocities is  $c$  and defined as  $c = \frac{b^*}{a^*}$  and  $\beta$  is constant, which gives a particular streamline.

In the absence of external mechanical body force, the flow equations are

$$\frac{\partial u^*}{\partial x} + \frac{\partial v^*}{\partial y} + \frac{\partial w^*}{\partial z} = 0, \quad (3.1)$$

$$u^* \frac{\partial u^*}{\partial x} + v^* \frac{\partial u^*}{\partial y} + w^* \frac{\partial u^*}{\partial z} = a^{*2}x + \left( \frac{\mu_{nf} + k}{\rho_{nf}} \right) \frac{\partial^2 u^*}{\partial z^2} - \frac{k}{\rho_{nf}} \frac{\partial N_2}{\partial z} - \frac{\sigma B_0^2}{\rho_{nf}} (u^* - a^*x), \quad (3.2)$$

$$u^* \frac{\partial v^*}{\partial x} + v^* \frac{\partial v^*}{\partial y} + w^* \frac{\partial v^*}{\partial z} = b^{*2}y + \left( \frac{\mu_{nf} + k}{\rho_{nf}} \right) \frac{\partial^2 v^*}{\partial z^2} + \frac{k}{\rho_{nf}} \frac{\partial N_1}{\partial z} - \frac{\sigma B_0^2}{\rho_{nf}} (v^* - b^*y), \quad (3.3)$$

$$u^* \frac{\partial T^*}{\partial x} + v^* \frac{\partial T^*}{\partial y} + w^* \frac{\partial T^*}{\partial z} = \alpha_{nf} \frac{\partial^2 T^*}{\partial z^2}, \quad (3.4)$$

$$u^* \frac{\partial N_1}{\partial x} + v^* \frac{\partial N_1}{\partial y} + w^* \frac{\partial N_1}{\partial z} = \frac{1}{\rho_{nf}} \left( \mu_{nf} + \frac{k}{2} \right) \frac{\partial^2 N_1}{\partial z^2} - \frac{2k}{j\rho_{nf}} \frac{\partial v^*}{\partial z} - \frac{2k}{j\rho_{nf}} N_1, \quad (3.5)$$

$$u^* \frac{\partial N_2}{\partial x} + v^* \frac{\partial N_2}{\partial y} + w^* \frac{\partial N_2}{\partial z} = \frac{1}{\rho_{nf}} \left( \mu_{nf} + \frac{k}{2} \right) \frac{\partial^2 N_2}{\partial z^2} + \frac{2k}{j\rho_{nf}} \frac{\partial u^*}{\partial z} - \frac{2k}{j\rho_{nf}} N_2. \quad (3.6)$$

The boundary conditions are

$$u^* = 0, v^* = 0, w^* = 0, N_1 = n \frac{\partial v^*}{\partial z}, N_2 = -n \frac{\partial u^*}{\partial z}, T^* = T_w^* \text{ at } z \rightarrow 0, \quad (3.7)$$

$$u^* \rightarrow a^*x, v^* \rightarrow b^*y, T \rightarrow T_\infty^*, N_1 \rightarrow 0, N_2 \rightarrow 0, \text{ at } z \rightarrow \infty. \quad (3.8)$$

where ‘ $u^*$ ’, ‘ $v^*$ ’ and ‘ $w^*$ ’ are the velocity components along  $x$ -,  $y$ - and  $z$ - direction respectively,  $B_0$  is the strength of magnetic field,  $T^*$  is the temperature distribution,  $N_1$  and  $N_2$  are the components of microrotation or angular velocity,  $\rho_{nf}$  is the density of nanofluid, nanofluids dynamic viscosity is  $\mu_{nf}$ ,  $k$  is the vortex viscosity,  $j$  is the microinertia coefficient,  $n$  is the micro-gyration parameter,  $T_w$  is the constant wall temperature,  $T_\infty$  is the ambient temperature,  $a^*$  and  $b^*$  are constant ( $> 0$ ). The nanofluid parameters are defined as

$$\mu_{nf} = \frac{\mu_f}{(1 - \phi)^{2.5}}, Pr = \frac{\nu}{\alpha}, \quad \rho_{nf} = (1 - \phi)\rho_f + \phi\rho_s,$$

$$\alpha_{nf} = \frac{\kappa_{nf}}{(\rho C_p)_{nf}}, (\rho C_p)_{nf} = (1 - \phi)(\rho C_p)_f + \phi(\rho C_p)_s,$$

$$\frac{\kappa_{nf}}{\kappa_f} = \frac{(\kappa_s + 2\kappa_f) - 2\phi((\kappa_s - \kappa_f))}{(\kappa_s + 2\kappa_f) + \phi((\kappa_s - \kappa_f))}.$$

Introducing the following similarities equations

$$u^* = a^*x f'(\eta), v^* = b^*y g'(\eta), w^* = -\sqrt{a^*u_f}(f + cg),$$

$$T^* = T_\infty^* + (T_w^* - T_\infty^*)\theta(\eta), \quad (3.9)$$

$$\eta = z\sqrt{\frac{v_f}{a^*}}, N_1 = b^*y\sqrt{\frac{a^*}{v_f}}h(\eta), N_2 = \sqrt{\frac{a^*}{v_f}}\psi(\eta).$$

With the help of the above equations, equation of continuity is identically satisfied while other equations take the following form

$$\left( \frac{1}{(1-\phi)^{2.5} \left(1-\phi+\phi \frac{\rho_s}{\rho_f}\right)} + \frac{K}{\left(1-\phi+\phi \frac{\rho_s}{\rho_f}\right)} \right) f''' + (f + cg)f'' - f'^2 - \frac{K}{\left(1-\phi+\phi \frac{\rho_s}{\rho_f}\right)} \psi' - \frac{M^2}{\left(1-\phi+\phi \frac{\rho_s}{\rho_f}\right)} (f' - 1) + 1 = 0, \quad 3.10$$

$$\left( \frac{1}{(1-\phi)^{2.5} \left(1-\phi+\phi \frac{\rho_s}{\rho_f}\right)} + \frac{K}{\left(1-\phi+\phi \frac{\rho_s}{\rho_f}\right)} \right) g''' + (f + cg)g'' - c g'^2 + \frac{K}{\left(1-\phi+\phi \frac{\rho_s}{\rho_f}\right)} h' - \frac{M^2}{\left(1-\phi+\phi \frac{\rho_s}{\rho_f}\right)} (f' - 1) + c = 0, \quad 3.11$$

$$\frac{\frac{K_{nf}}{\kappa_f}}{\text{Pr} \left( 1 - \phi + \phi \frac{(\rho C_p)_s}{(\rho C_p)_f} \right)} \theta'' + (f + cg)\theta' = 0, \quad 3.12$$

$$\left( \frac{1}{(1-\phi)^{2.5} \left(1-\phi+\phi \frac{\rho_s}{\rho_f}\right)} + \frac{K}{2 \left(1-\phi+\phi \frac{\rho_s}{\rho_f}\right)} \right) h'' + (f + cg)h' - \frac{2K}{\left(1-\phi+\phi \frac{\rho_s}{\rho_f}\right)} h - \frac{K}{\left(1-\phi+\phi \frac{\rho_s}{\rho_f}\right)} g'' - cg'h = 0, \quad 3.13$$

$$\left( \frac{1}{(1-\phi)^{2.5} \left(1-\phi+\phi \frac{\rho_s}{\rho_f}\right)} + \frac{K}{2 \left(1-\phi+\phi \frac{\rho_s}{\rho_f}\right)} \right) \psi'' + (f + cg)\psi' - \left( \frac{2K}{\left(1-\phi+\phi \frac{\rho_s}{\rho_f}\right)} \psi + \frac{K}{\left(1-\phi+\phi \frac{\rho_s}{\rho_f}\right)} f'' - f'\psi \right) = 0. \quad 3.14$$

Respectively boundary conditions are

$$\begin{aligned}
f(0) = 0, f'(0) = 0, f'(\infty) = 1, g(0) = 0, g'(0) = 0, g'(\infty) = 1, \theta(0) = 1, \\
\theta(\infty) = 0, h(0) = ng''(0), h(\infty) = 0, \psi(0) = -nf''(0), \psi(\infty) = 0.
\end{aligned} \tag{3.15}$$

Where,  $h$  and  $\psi$  are dimensionless angular velocities, the temperature profile is  $\theta$ ,  $f$ , and  $g$  are function related to the velocity field and the primes denote differentiation with respect to  $\eta$ .

### 3.3 Nusselt number and Skin friction coefficient

Two main essential physical quantities of present research are skin friction coefficient  $C_{fx}$  and  $C_{fy}$  in the direction of  $x$  – and  $y$  – axis respectively and the local Nusselt number. Which are characterize as below

$$C_{fx} = \frac{\tau_{wx}}{\rho_f u_w^2}, \quad C_{fy} = \frac{\tau_{wy}}{\rho_f u_w^2}, \quad Nu_x = \frac{xq_w}{k_f(T_w - T_\infty)}, \tag{3.3.1}$$

These equations  $\tau_{wx}$  and  $\tau_{wy}$  are the shear stress surface in the  $x$  – and  $y$  – directions respectively. The surface heat flux is denoted as  $q_w$ , defined as below

$$\begin{aligned}
\tau_{wx} = [(\mu_{nf}/\mu_f + k) \frac{\partial u^*}{\partial z} + kN_2]_{z=0}, \tau_{wy} = [(\mu_{nf}/\mu_f + k) \frac{\partial v^*}{\partial z} + kN_1]_{z=0}, \\
q_w = -k_{nf} \left( \frac{\partial T^*}{\partial z} \right)_{z=0},
\end{aligned} \tag{3.3.2}$$

From equation (3.3.1) and (3.3.2), we get it

$$\begin{aligned}
Re_x^{1/2} C_{fx} &= \left( \frac{1}{(1-\phi)^{2.5}} + (1-n)K \right) f''(0), \\
(x/y) Re_x^{-1/2} C_{fy} &= c \left( \frac{1}{(1-\phi)^{2.5}} + (1+n)K \right) g''(0), \\
Re_x^{-1/2} Nu_x &= -\frac{k_{nf}}{k_f} \theta'(0).
\end{aligned}$$

where  $Re = \frac{ax}{v_{nf}}$  is the local Reynolds number.

### 3.4 Results and discussion

Numerical solutions of Eqs. (3.10 – 3.15) have been solved numerically by using fifth order Runge-Kutta-Fehlberg method. The nanofluids velocity profiles are shown in Figs. (3.1 – 3.6). Generally, the flow over a cylinder is driven by the combined action of magnetic field and free stream velocity. The nanofluids velocity is zero at both saddle and nodal point on the cylinder and increase gradually until it attain the free stream velocity far away from the cylinder, satisfying the prescribed boundary conditions. In the present study, we are discussed namely alumina ( $Al_2O_3$ ), titania ( $TiO_2$ ), and copper (Cu). The thermophysical properties of water and the nanoparticles Cu,  $Al_2O_3$  and  $TiO_2$  are shown in **Table 2.1**. In order to validate the accuracy of our numerical procedure, the special case of nanoparticles in the presence of Hartmann number is noted as revealed in **Table 3.1**, our study work agreed perfectly with S. Dinarvand et al. [30].

<b>Table 3.1.</b> Comparison with [30] for the values of $Re_x^{1/2}C_{fx}$ , $Re_x^{1/2}C_{fy}$ and $Re_x^{-1/2}Nu_x$ when $K = 0, M = 0$ .							
	$\phi$	$Re_x^{1/2}C_{fx}$		$Re_x^{1/2}C_{fy}$		$Re_x^{-1/2}Nu_x$	
		[30]	Present	[30]	Present	[30]	Present
Cu	0.0	1.2681	1.2678	0.4993	0.4991	1.3301	1.3299
	0.1	1.9387	1.9386	0.7630	0.7627	1.6185	1.6183
	0.2	2.6968	2.6966	1.0617	1.0616	1.9293	1.9293
$Al_2O_3$	0.0	1.2681	1.2678	0.4993	0.4991	1.3301	1.3298
	0.1	1.6482	1.6480	0.6487	0.6485	1.5726	1.5725
	0.2	2.1176	2.1175	0.8334	0.8333	1.8172	1.8171
$TiO_2$	0.0	1.2681	1.2678	0.4993	0.4991	1.3301	1.3298
	0.1	1.6657	1.6656	0.6557	0.6556	1.4956	1.4955
	0.2	2.1530	2.1528	0.8477	0.8774	1.7386	1.7385

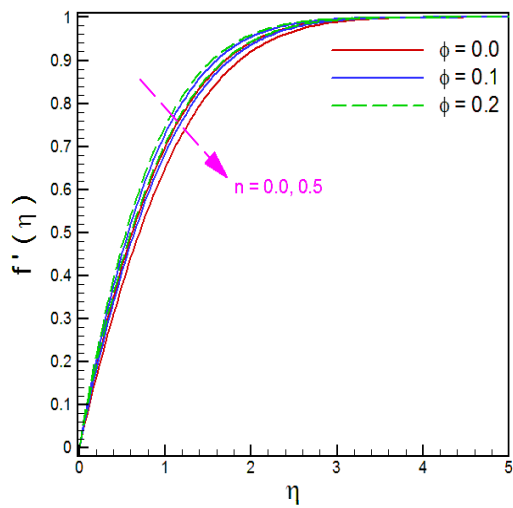
**Figs. (3.1-3.6)**, depict velocity distributions ( $f'(\eta)$  and  $g'(\eta)$ ), angular velocity distributions ( $\psi(\eta)$  and  $h(\eta)$ ) and temperature distribution  $\theta(\eta)$  viz  $\eta$ . **Figs. (3.1-3.3)** and **Fig. (3.6)** report the



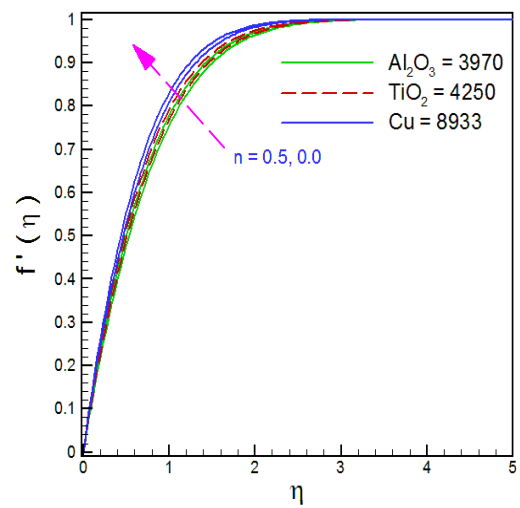
behavior of dimensionless nanofluids velocities ( $f'(\eta)$  and  $g'(\eta)$ ) and angular velocities ( $\psi(\eta)$  and  $h(\eta)$ ) for various value of physical parameter namely magnetic field parameter  $M$ , solid densities of nanoparticles ( $\text{Al}_2\text{O}_3, \text{TiO}_2$  and  $\text{Cu}$ )  $\rho_s$ , nanoparticles volume fractions  $\phi$ , microgyration parameter  $n$  and material parameter  $K$ . It is seen that for the different value of physical parameters  $\phi$ ,  $K$ ,  $M$  and  $n$ , the nanofluid velocity distributions  $f'(\eta)$  and  $g'(\eta)$  and angular velocity distribution  $h(\eta)$  increase due to increase in the solid nanoparticles and magnetic field but change the behavior of micropolar parameter and  $n$  opposite at particular point of the flow region. **Fig. 3.1** (d), **Fig. 3.2** (d) and **Fig. 3.6** (d) depict flow field of velocities  $f'(\eta)$  and  $g'(\eta)$  and angular velocity profiles  $h(\eta)$  are reduced due to rising the value of  $\phi$  and  $M$  but change the behavior opposite for  $K$  and  $n$ . The results have shown that increment of  $\phi$  and  $M$  produce a large heat transfer effect at  $n = 0.0$  and  $n = 0.5$  but reduced for large value of  $K$  and  $n$ . Further it is found from **Fig. 3.3** (a) and **Fig. 3.3** (c) which the micropolar distribution decreases due to increment in the physical parameters  $\phi$  and  $M$  at  $n = 0.0$  and  $n = 0.5$ . In **Fig. 3.3** (d) shows that the micropolar distribution increases with an increase in micropolar parameter  $K$ . **Fig. 3.4** (a) and **Fig. 3.4** (b) exhibit the temperature distribution in the absence of solid nanoparticle  $\phi$  and solid density of nanoparticles ( $\text{Al}_2\text{O}_3, \text{TiO}_2$  and  $\text{Cu}$ )  $\rho_s$ . **Fig. 3.4**(a) depicts flow field of temperature profile  $\theta(\eta)$  is increased with the increment of  $\phi$  but reduced when increase the value of  $n$ . The effect of  $\phi$  and  $M$  are seen to maximum of the micropolar profile (angular velocity) at surface, which reduces the angular velocity profile at surface when increase  $n$  and  $K$ , are shown in **Fig. 3.6** (a), **Fig. 3.6** (c) and **Fig. 3.6** (d). It is seen that velocity, angular velocity and temperature distributions are enhanced at saddle and nodal points, shown in **Fig. 3.5**. Besides, it demonstrates copper-water and alumina-water nanofluids have the lowest and highest velocities, angular velocities and temperature distributions respectively at  $n = 0.0$  and  $n = 0.5$  but change the

behavior opposite of angular velocities distributions, shown in **Fig. 3.5 (b)**. It is noted that increased the values of  $n$  decrease in velocity, angular velocity, and temperature distributions

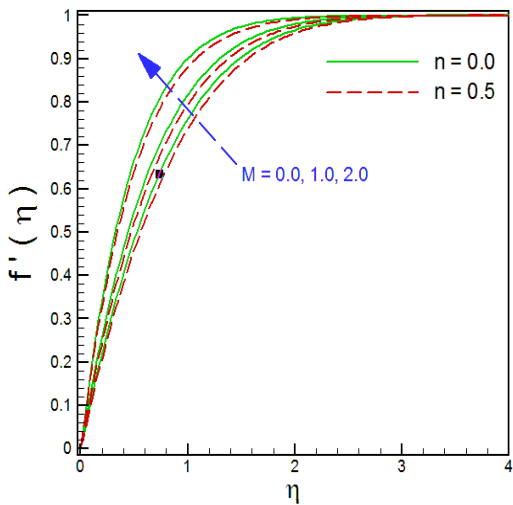
The numerical values of Skin frictions and Nusselt numbers for different parameter  $K$ ,  $M$ ,  $\phi$ ,  $n$  and  $c$  are shown in **Tables** [3.2 – 3.4]. It is observed that temperature gradient reduces with the increment of volume friction  $\phi$ , micropolar parameter  $K$ , and slip parameter  $n$  but opposite results of magnetic field  $M$  and heat transfer rate increased due to increment in physical parameters ( $\phi$  and  $M$ ) at the surface of cylinder which shown in table **Tables** [3.2 – 3.4]. From the **Tables** [3.2 – 3.4], boundary layer thickness enhanced with enhance in  $\phi$  and  $M$  but declined due to large values of  $n$  and  $k$  near the surface of cylinder. It is very interesting results that the highest rate of heat transfer is achieved for the Cu nanoparticles. The nanoparticles of Cu have the largest value of thermal conductivity compared with  $Al_2O_3$  and  $TiO_2$  in both cases when  $n = 0$  and  $n = 0.5$ . Therefore, decreased value of thermal diffusivity leads to high increases in heat transfer and high temperature gradient. The nanoparticles of Cu have high values of thermal diffusivity. The nanoparticles volume fraction is enhanced from 0 to 0.2. We can observed that is the largest improvement in the Nusselt number for the Cu nanoparticles. The nanoparticles Titania ( $TiO_2$ ) is achieved minimum heat transfer rate. This is considering  $TiO_2$  has the least value of thermal conductivity in comparison with Cu and  $Al_2O_3$ .



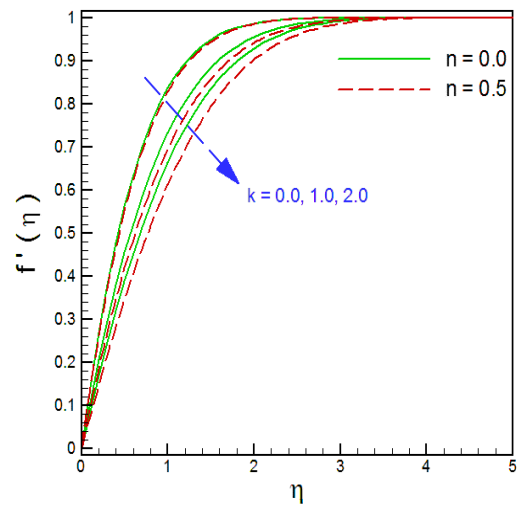
(a)



(b)

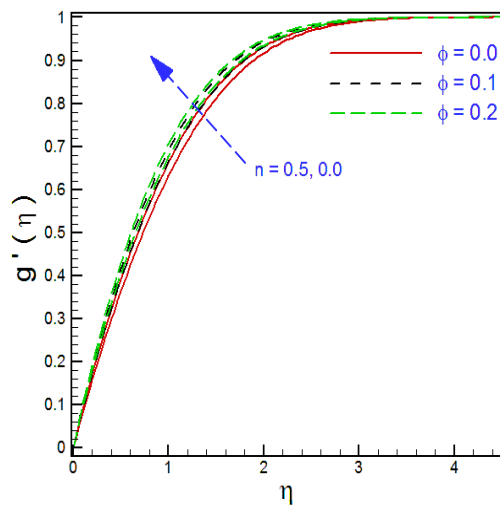


(d)

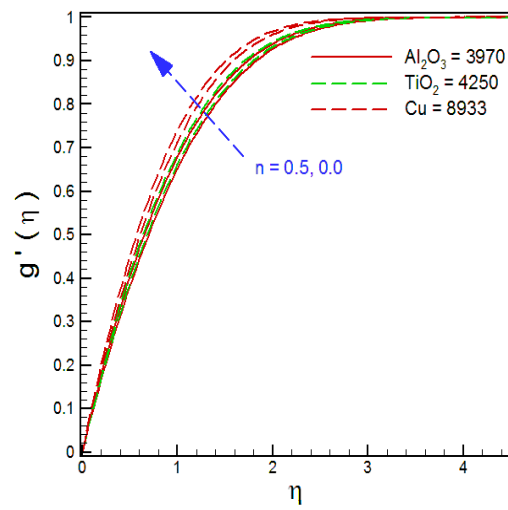


(e)

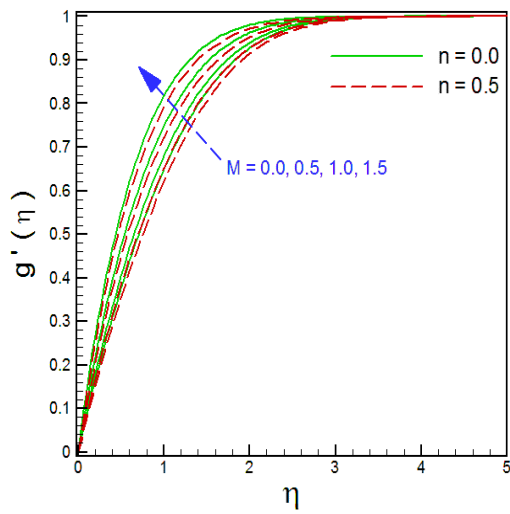
**Fig. (3.1).** Plots showing the behavior of  $f'(\eta)$  for different physical parameters  $\phi$ ,  $K$ ,  $M$  and  $\rho_s$ .



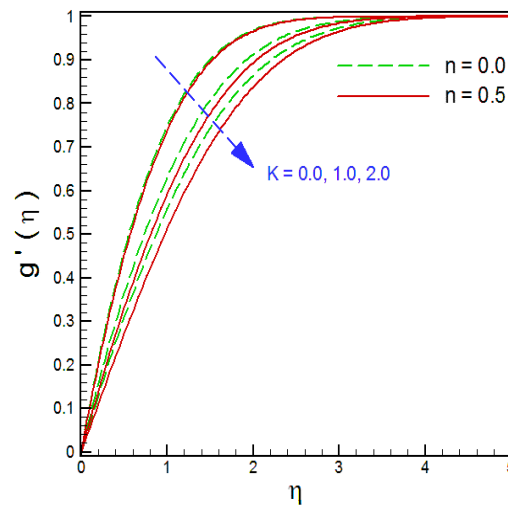
(a)



(b)

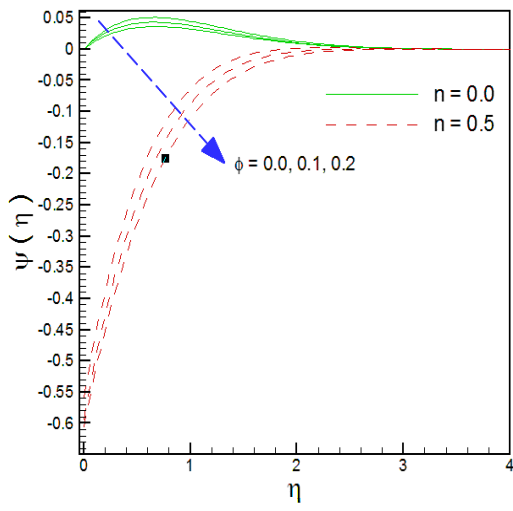


(c)

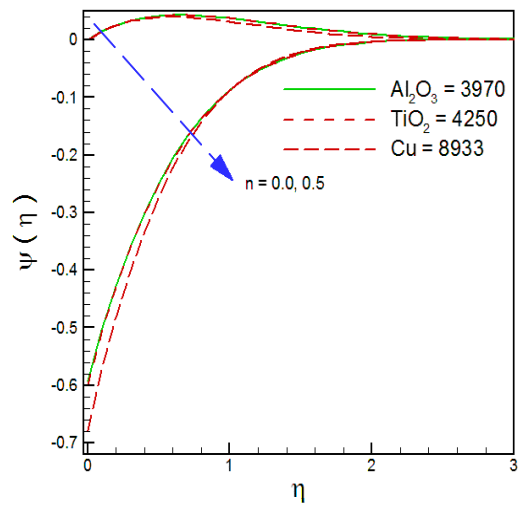


(d)

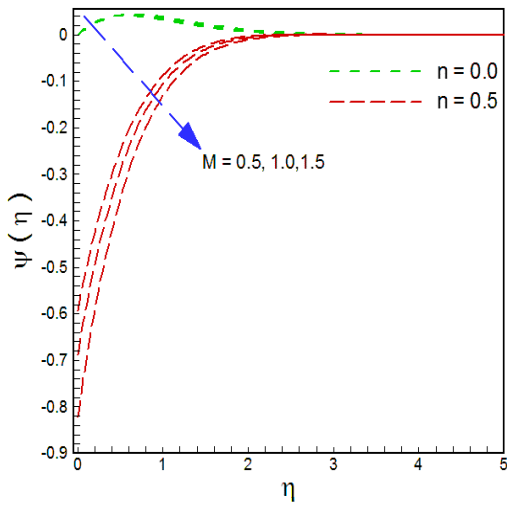
**Fig. (3.2).** Plots showing the behavior of  $g'(\eta)$  for different physical parameters  $\phi$ ,  $K$ ,  $M$  and  $\rho_s$ .



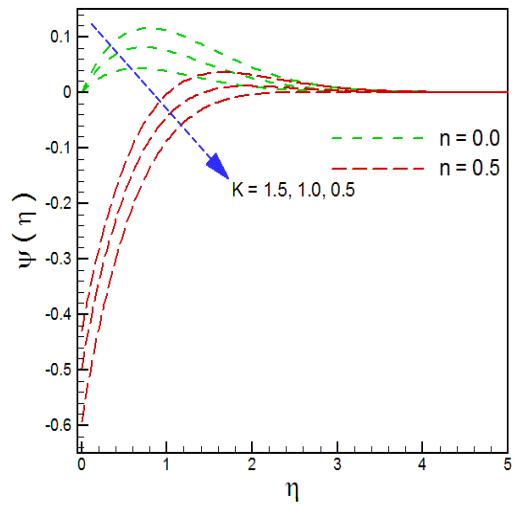
(a)



(b)

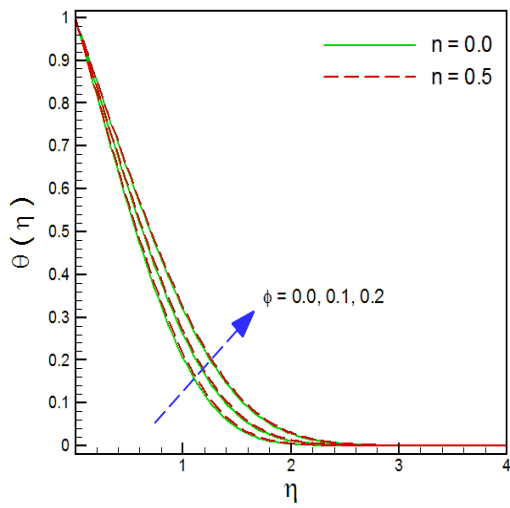


(c)

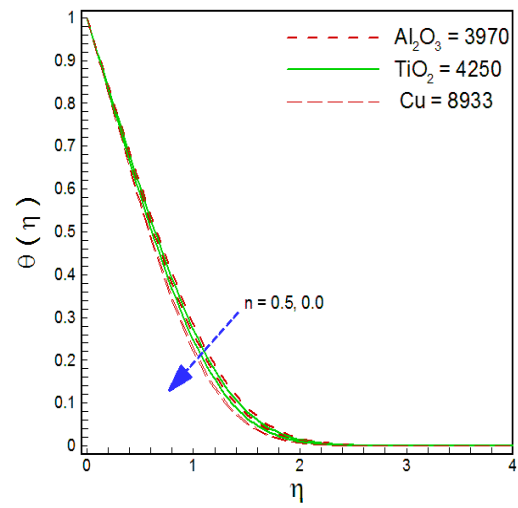


(d)

**Fig. (3.3).** Plots showing the behavior of  $\psi(\eta)$  for different physical parameters  $\phi$ ,  $K$ ,  $M$  and  $\rho_s$ .

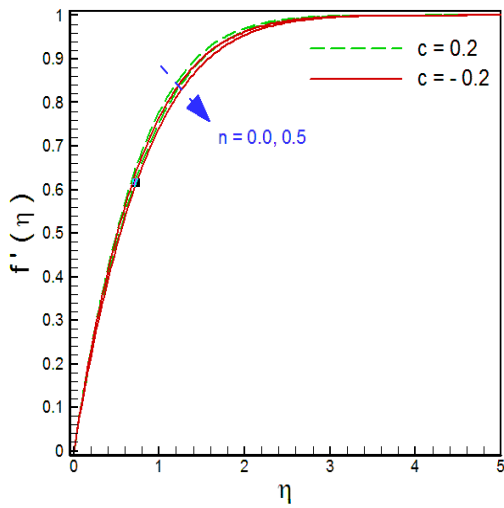


(a)

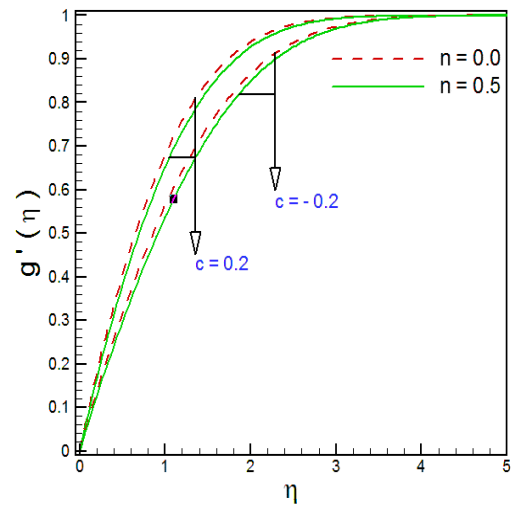


(b)

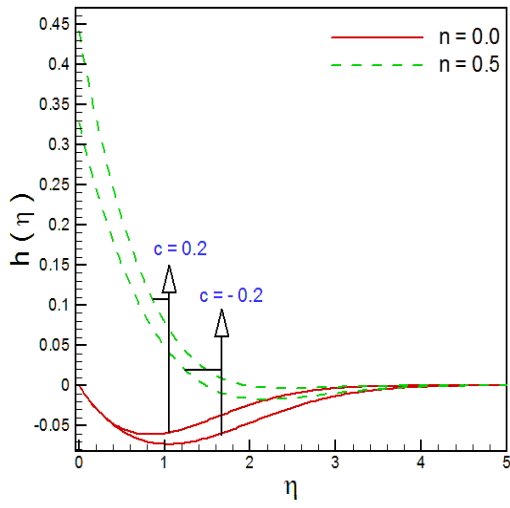
**Fig. (3.4).** Plots showing the behavior of  $\theta(\eta)$  for different physical parameters  $\phi$  and  $\rho_s$ .



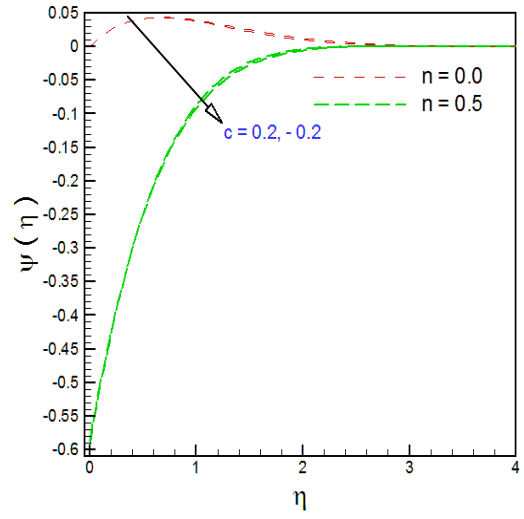
(a)



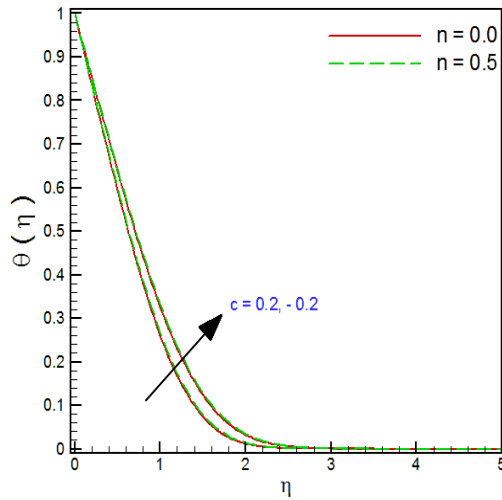
(b)



(c)

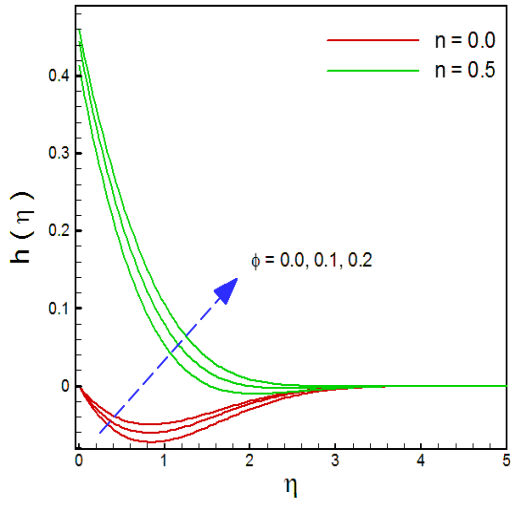


(d)

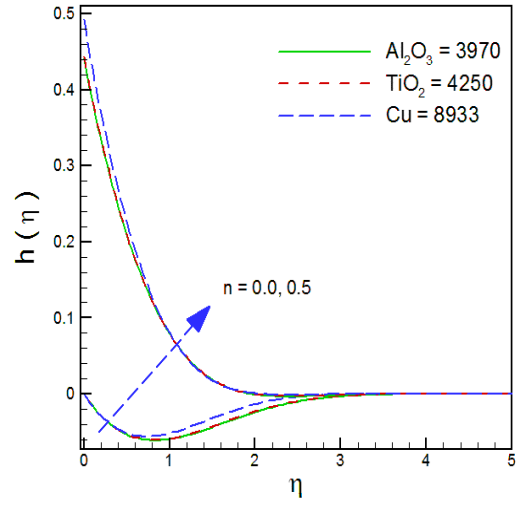


(e)

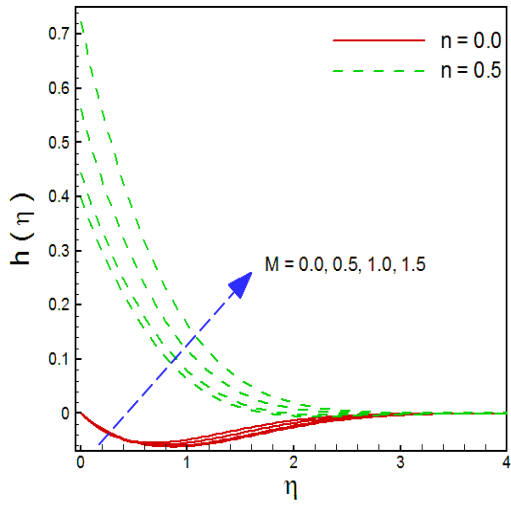
**Fig. (3.5).** Impact of  $c$  on velocity, angular velocity and temperature profiles at saddle and nodal points.



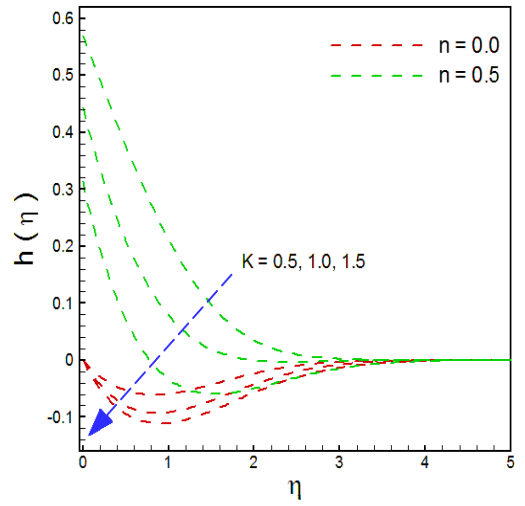
(a)



(b)



(c)



(d)

**Fig. (3.6).** Plots showing the behavior of  $h(\eta)$  for different physical parameters  $\phi$ ,  $K$ ,  $M$  and  $\rho_s$ .



<b>Table 3.2.</b> Numerical value $f''(0)$ , $g''(0)$ and $-\theta'(0)$ for K, M, $\phi$ and n for $\text{TiO}_2$ – water								
TiO <sub>2</sub> – water			n = 0.0			n = 0.5		
$\phi$	K	M	$f''(0)$	$g''(0)$	$-\theta'(0)$	$f''(0)$	$g''(0)$	$-\theta'(0)$
0.0	0.5	0.5	1.0836	0.7207	1.1430	0.9813	0.6479	1.1158
0.1			1.1425	0.7624	1.0539	1.0546	0.6989	1.0335
0.2			1.1444	0.7653	0.9608	1.0748	0.7145	0.9462
0.1	0.0		1.3534	0.9087	1.1031	1.3534	0.9087	1.1031
	0.5		1.1425	0.7624	1.0539	1.0546	0.6989	1.0335
	1.0		0.9949	0.6601	1.0168	0.8780	0.5716	0.9864
	1.5		0.8827	0.5857	0.9868	0.7566	0.4876	0.9510
	0.5	0.0	1.0597	0.6442	1.0322	0.9753	0.5861	1.0118
		0.5	1.1425	0.7624	1.0539	1.0546	0.6989	1.0335
		1.0	1.3611	1.0501	1.1042	1.2649	0.9754	1.0840
		1.5	1.6634	1.4140	1.1619	1.5571	1.3283	1.1422

<b>Table 3.3</b> Numerical value $f''(0)$ , $g''(0)$ and $-\theta'(0)$ for K, M, $\phi$ and n for Cu – water.								
Cu – water			n = 0.0			n = 0.5		
$\phi$	K	M	$f''(0)$	$g''(0)$	$-\theta'(0)$	$f''(0)$	$g''(0)$	$-\theta'(0)$
0.0	0.5	0.5	1.0836	0.7207	1.1430	0.9813	0.6479	1.1158
0.1			1.3313	0.8896	1.0851	1.2320	0.8171	1.0649
0.2			1.4352	0.9610	0.9960	1.3514	0.8989	0.9817
0.1	0.0		1.5749	1.0574	1.1342	1.5749	1.0574	1.1342
	0.5		1.3313	0.8896	1.0851	1.2320	0.8171	1.0649
	1.0		1.1630	0.7728	1.0482	1.0303	0.6720	1.0180
	1.5		1.0364	0.6875	1.0185	0.8925	0.5753	0.9826
	0.5	0.0	1.2350	0.7520	1.0637	1.1395	0.6855	1.0435
		0.5	1.3313	0.8896	1.0851	1.2320	0.8171	1.0649
		1.0	1.5857	1.2245	1.1347	1.4773	1.1398	1.1148
		1.5	1.9375	1.6480	1.1914	1.8182	1.5512	1.1720

<b>Table: 3.4</b> Numerical value $f''(0), g''(0)$ and $-\theta'(0)$ for K, M, $\phi$ and n for $Al_2O_3 - water$								
$Al_2O_3 - water$			n = 0.0			n = 0.5		
$\phi$	K	M	$f''(0)$	$g''(0)$	$-\theta'(0)$	$f''(0)$	$g''(0)$	$-\theta'(0)$
0.0	0.5	0.5	1.0836	0.7207	1.1430	0.9813	0.6479	1.1158
0.1			1.1320	0.7541	1.0376	1.0431	0.6912	1.0176
0.2			1.1247	0.7620	0.9333	1.0560	0.7020	0.9191
0.1	0.0		1.3390	0.8990	1.0860	1.3390	0.8990	1.0860
	0.5		1.1302	0.7541	1.0376	1.0431	0.6912	1.0176
	1.0		0.9840	0.6527	1.0011	0.8681	0.5651	0.9712
	1.5		0.8728	0.5791	0.9716	0.7478	0.4819	0.9364
	0.5	0.0	1.0483	0.6371	1.0163	0.9646	0.5797	0.9963
		0.5	1.1302	0.7541	1.0376	1.0431	0.6912	1.0176
		1.0	1.3465	1.0387	1.0870	1.2511	0.9648	1.0672
		1.5	1.6456	1.3988	1.1437	1.5401	1.3138	1.1243

### 3.5 Final remarks

We discussed the effects of MHD micropolar nanofluid in the presence of stagnation point flow over a circular cylinder having sinusoidal radius variation by using Runge-Kutta-Fehlberg method. In this article, three various types of nanoparticles are studied, especially alumina, titania and copper with base fluid water. The present results of influence are noted.

- Velocity distributions enhance for large values of different parameters viz  $M$ ,  $\phi$  and  $\rho_s$  and reduce for large values of  $K$ .
- Large values of different parameters viz  $M$ ,  $\phi$  and  $\rho_s$  show the same behavior on micropolar profile  $h(\eta)$  while opposite attitude toward  $K$ .
- The micropolar profile  $\psi(\eta)$  increased with increase  $M$ ,  $\phi$  and  $\rho_s$  but decreased due to enhance in  $K$ .
- Temperature distribution is increased for large values of solid nanoparticle  $\phi$  but decreases with increase in  $\rho_s$ .
- We are investigated the impact of the micro-gyration parameter  $n$  on the Nusselt number and skin friction coefficients reduce with soar in  $n$ .
- Skin friction coefficient and Nusselt number increase for large values of  $\phi$  for various nanoparticles namely as  $Al_2O_3$ ,  $TiO_2$  and  $Cu$ .
- The best heat carried  $Cu$  as compare to others  $Al_2O_3$  and  $TiO_2$ . But  $TiO_2$  proved to be lower rate heat transfer than other.
- All the descriptive quantities of the flow as compared to the Newtonian case, the nature of micropolar fluid decreases.

### 3.6 References

1. Chol, S. U. S. (1995). Enhancing thermal conductivity of fluids with nanoparticles. *ASME-Publications-Fed*, 231, 99-106.
2. Buongiorno, J. (2006). Convective transport in nanofluids. *Journal of Heat Transfer*, 128(3), 240-250.
3. Khan, W. A., & Pop, I. (2010). Boundary-layer flow of a nanofluid past a stretching sheet. *International journal of heat and mass transfer*, 53(11), 2477-2483.
4. Turkyilmazoglu, M., & Pop, I. (2013). Heat and mass transfer of unsteady natural convection flow of some nanofluids past a vertical infinite flat plate with radiation effect. *International Journal of Heat and Mass Transfer*, 59, 167-171.
5. Nadeem, S., & Lee, C. (2012). Boundary layer flow of nanofluid over an exponentially stretching surface. *Nanoscale Research Letters*, 7(1), 94.
6. Eringen, A. C. (1966). Theory of micropolar fluids. *Journal of Mathematics and Mechanics*, 1-18.
7. Eringen, A. C. (1972). Theory of thermomicrofluids. *Journal of Mathematical Analysis and Applications*, 38(2), 480-496.
8. Bourantas, G. C., & Loukopoulos, V. C. (2014). Modeling the natural convective flow of micropolar nanofluids. *International Journal of Heat and Mass Transfer*, 68, 35-41.
9. Buongiorno, J. (2006). Convective transport in nanofluids. *Journal of Heat Transfer*, 128(3), 240-250.
10. Ashraf, M., & Ashraf, M. M. (2011). MHD stagnation point flow of a micropolar fluid towards a heated surface. *Applied Mathematics and Mechanics*, 32(1), 45-54.

11. Nazar, R., Amin, N., Filip, D., & Pop, I. (2004). Stagnation point flow of a micropolar fluid towards a stretching sheet. *International Journal of Non-Linear Mechanics*, 39(7), 1227-1235.
12. Yücel, A. (1989). Mixed convection in micropolar fluid flow over a horizontal plate with surface mass transfer. *International Journal of Engineering Science*, 27(12), 1593-1602.
13. Lok, Y. Y., Amin, N., Campean, D., & Pop, I. (2005). Steady mixed convection flow of a micropolar fluid near the stagnation point on a vertical surface. *International Journal of Numerical Methods for Heat & Fluid Flow*, 15(7), 654-670.
14. Alomari, A. K., Noorani, M. S. M., & Nazar, R. (2011). Homotopy solution for flow of a micropolar fluid on a continuous moving surface. *International Journal for Numerical Methods in Fluids*, 66(5), 608-621.
15. Ishak, A., Lok, Y. Y., & Pop, I. (2010). Stagnation-point flow over a shrinking sheet in a micropolar fluid. *Chemical Engineering Communications*, 197(11), 1417-1427.
16. Yacob, N. A., & Ishak, A. (2011). MHD flow of a micropolar fluid towards a vertical permeable plate with prescribed surface heat flux. *Chemical Engineering Research and Design*, 89(11), 2291-2297.
17. Takhar, H. S., Agarwal, R. S., Bhargava, R., & Jain, S. (1998). Mixed convection flow of a micropolar fluid over a stretching sheet. *Heat and Mass Transfer*, 34(2), 213-219.
18. Rauf, A., Ashraf, M., Batool, K., Hussain, M., & Meraj, M. A. (2015). MHD flow of a micropolar fluid over a stretchable disk in a porous medium with heat and mass transfer *AIP Advances*, 5(7), 077156.

19. Siddiq, M. K., Rauf, A., Shehzad, S. A., Abbasi, F. M., & Meraj, M. A. (2017). Thermally and solutally convective radiation in MHD stagnation point flow of micropolar nanofluid over a shrinking sheet. *Alexandria Engineering Journal*.
20. Sheikholeslami, M., Hatami, M., & Ganji, D. D. (2014). Micropolar fluid flow and heat transfer in a permeable channel using analytical method. *Journal of Molecular Liquids*, 194, 30-36.
21. Borrelli, A., Giantesio, G., & Patria, M. C. (2013). Numerical simulations of three-dimensional MHD stagnation-point flow of a micropolar fluid. *Computers & Mathematics with Applications*, 66(4), 472-489.
22. Wang, C. Y. (2008). Similarity stagnation point solutions of the Navier–Stokes equations—review and extension. *European Journal of Mechanics-B/Fluids*, 27(6), 678-683.
23. Hiemenz, K. (1911). Die Grenzschicht an einem in den gleichförmigen Flüssigkeitsstrom eingetauchten geraden Kreiszynder. *Dinglers J.*, 326, 321-324.
24. Homann, F. (1936). Der Einfluss grosser Zähigkeit bei der Strömung um den Zylinder und um die Kugel. *ZAMM-Journal of Applied Mathematics and Mechanics/Zeitschrift für Angewandte Mathematik und Mechanik*, 16(3), 153-164.
25. Nazar, R., Amin, N., Filip, D., & Pop, I. (2004). Unsteady boundary layer flow in the region of the stagnation point on a stretching sheet. *International Journal of Engineering Science*, 42(11), 1241-1253.
26. Haq, R. U., Nadeem, S., Khan, Z. H., & Akbar, N. S. (2015). Thermal radiation and slip effects on MHD stagnation point flow of nanofluid over a stretching sheet. *Physica E: Low-dimensional Systems and Nanostructures*, 65, 17-23.

27. Akbar, N. S., Nadeem, S., Haq, R. U., & Khan, Z. H. (2013). Radiation effects on MHD stagnation point flow of nano fluid towards a stretching surface with convective boundary condition. *Chinese Journal of Aeronautics*, 26(6), 1389-1397.
28. Nazar, R., Amin, N., Filip, D., & Pop, I. (2004). Unsteady boundary layer flow in the region of the stagnation point on a stretching sheet. *International Journal of Engineering Science*, 42(11), 1241-1253.
29. Oztop, H. F., & Abu-Nada, E. (2008). Numerical study of natural convection in partially heated rectangular enclosures filled with nanofluids. *International journal of heat and fluid flow*, 29(5), 1326-1336.
30. Dinarvand, S., Hosseini, R., Damangir, E., & Pop, I. (2013). Series solutions for steady three-dimensional stagnation point flow of a nanofluid past a circular cylinder with sinusoidal radius variation. *Meccanica*, 48(3), 643-652.
31. Yazdi, M. E., Nejad, A. K., Dinarvand, S., & Tamim, H. (2014). Brownian Motion Effects on Natural Convection of Alumina–Water Nanofluid in 2-D Enclosure. *Heat Transfer—Asian Research*, 43(8), 720-733.